

Communication

Lattice Resonances in Transdimensional WS₂ Nanoantenna Arrays

Viktoriia E. Babicheva *  and Jerome V. Moloney

College of Optical Sciences, University of Arizona, Tucson, AZ 85721, USA; jml@acms.arizona.edu

* Correspondence: vbb@unm.edu

Received: 1 April 2019; Accepted: 14 May 2019; Published: 16 May 2019

**Featured Application:** ultra-thin optical components, metasurfaces.

Abstract: Mie resonances in high-refractive-index nanoparticles have been known for a long time but only recently have they become actively explored for control of light in nanostructures, ultra-thin optical components, and metasurfaces. Silicon nanoparticles have been widely studied mainly because of well-established fabrication technology, and other high-index materials remain overlooked. Transition metal dichalcogenides, such as tungsten or molybdenum disulfides and diselenides, are known as van der Waals materials because of the type of force holding material layers together. Transition metal dichalcogenides possess large permittivity values in visible and infrared spectral ranges and, being patterned, can support well-defined Mie resonances. In this *Communication*, we show that a periodic array of tungsten disulfide (WS₂) nanoantennae can be considered to be transdimensional lattice and supports different multipole resonances, which can be controlled by the lattice period. We show that lattice resonances are excited in the proximity to Rayleigh anomaly and have different spectral changes in response to variations of one or another orthogonal period. WS₂ nanoantennae, their clusters, oligomers, and periodic array have the potential to be used in future nanophotonic devices with efficient light control at the nanoscale.

Keywords: transition metal dichalcogenides; Mie resonances; multipole resonances; collective effects; two-dimensional materials; nanomaterials; transdimensional lattices; van der Waals materials

1. Introduction

Nanoparticles and nanoantennae resulting from subwavelength patterning of single- and multi-layer structures have been shown to be an effective way to control light at the nanoscale. High-refractive-index nanoparticles support excitation of multipole Mie resonances of different orders whose strength is mainly defined by the nanoparticle size, index of the material, and ohmic losses. While nanoparticles with moderate refractive index $n \approx 1.45$ –2 (e.g., silicon oxide and nitride) have resonances with relatively high radiative losses and low quality factors, materials with $n > 3.5$ (e.g., silicon) enable high mode localization and relatively low radiative losses. Multipole resonances in high-index nanoparticles are comparable to resonances in plasmonic [1] and hyperbolic nanostructures [2,3], as the main role is played by the index difference at the nanoparticle surface.

So far, most of the studies have dealt with silicon [4–8] or III-V nanoantennae [9] because of the readily available fabrication processes and well-established technology. However, recently emerging two-dimensional and layered materials hold great promise to be applied in next-generation optoelectronic devices and more efficient light harvesting [10–12]. Transition metal dichalcogenides (TMDCs), such as tungsten or molybdenum disulfides and diselenides (WS₂, MoS₂, WSe₂, MoSe₂) and others, are van der Waals layered materials with high anisotropy, exciton resonances in the visible spectral range, strong nonlinear response, and tunability. Layered material anisotropy results in

different in-plane and out-of-plane permittivity components, and the excitons in visible range result in a large imaginary part of the permittivity along with the increased real part. A large imaginary part not only causes non-radiative losses but also facilitates excitation of Zenneck modes and light confinement within the guiding nanolayer [13] or nanoparticles [14]. In the near-infrared range, the losses in TMDCs are near zero, and the nanoparticle can support Mie resonances with high quality factor [15]. Nanoparticle array can be fabricated by patterning TMDC layer (or flakes) using electron-beam exposure of a negative resist and dry etching, see e.g., [15]. An overview of fabrication techniques of transition metal dichalcogenides heterostructure systems can be found in [16].

Nanoparticle resonances can be enhanced, and their spectral position can be controlled not only by the nanoparticle size, shape, and material but also their arrangement in the clusters and/or lattices [17–24]. Nanoparticle clusters facilitate excitation of narrow Fano resonances [1] that are very sensitive to the parameter changes, can be easily tuned in the spectral domain or lost because of the imperfections. In contrast, the periodical arrangement of nanoparticles in the lattice enables excitation of lattice resonances that have a relatively high tolerance to local imperfections. The spectral position of different multipoles can be controlled by mutually perpendicular periods of the nanoparticle array [25,26].

In this work, we report on the theoretical prediction of Mie resonances in a periodic array of WS₂ nanodisks and their control by the lattice dimensions. We show excitation of multipole resonances in the proximity to the Rayleigh anomaly λ_{RA} (wavelength equal to the product of surrounding refractive index n and array period $p_{x,y}$, $\lambda_{\text{RA}} = np_{x,y}$) and a different optical response depending on the period changes in such a transdimensional lattice. The lattice resonances can be observed as a peak in reflection and absorption at the wavelength $\lambda \approx \lambda_{\text{RA}} = np_{x,y}$. Because of the high real part of WS₂ in-plane permittivity tensor component in the near-infrared range, the lattice resonance of the electric dipole is excited even for large and elongated periodic cells ($240 \times 700 \text{ nm}^2$).

2. Results

We consider a periodic rectangular array of WS₂ nanodisks surrounded by a uniform medium with moderate refractive index $n = 1.5$ (equivalent to matched-index substrate and superstrate, Figure 1a). Permittivity components of WS₂ are presented in Figure 1b where ϵ_{\parallel} is in-plane and ϵ_{zz} is out-of-plane tensor components and $\epsilon_{\text{WS}_2} = (\epsilon_{\parallel}, \epsilon_{\parallel}, \epsilon_{zz})$. One can see that losses of ϵ_{\parallel} are relatively high for $\lambda < \lambda_c = 655 \text{ nm}$, and nanoparticle resonances in this spectral region are not well defined for a dense array. At the same time, for $\lambda > \lambda_c$, the absorption peak is clearly seen for the electric dipole (ED) resonance $\lambda_{\text{ED}} \approx 697 \text{ nm}$ (Figure 1c, red line and Figure 1d), which indicates excitation of Mie resonance. The E-field profile at $\lambda = 697 \text{ nm}$ in Figure 1d is not the one of a pure ED multipole but the distribution is clearly seen with the main contribution of ED resonance. Absorption is calculated as losses in the nanoparticle regardless of the number of diffraction orders taken into account, and the resonance is associated with an increase in reflection at the wavelength about 690 nm (Figure 1c, blue line).

We analyze the absorption and reflection properties in the transdimensional lattice [27] with different periods in orthogonal direction p_x and p_y . In numerical modeling, we consider the normal incidence of light, one WS₂ nanodisk in the unit cell, periodic boundary conditions in x - and y -directions, and the artificial perfectly matched layers in the z -direction. We perform numerical simulations with finite element method implemented in CST Microwave Studio frequency-domain solver.

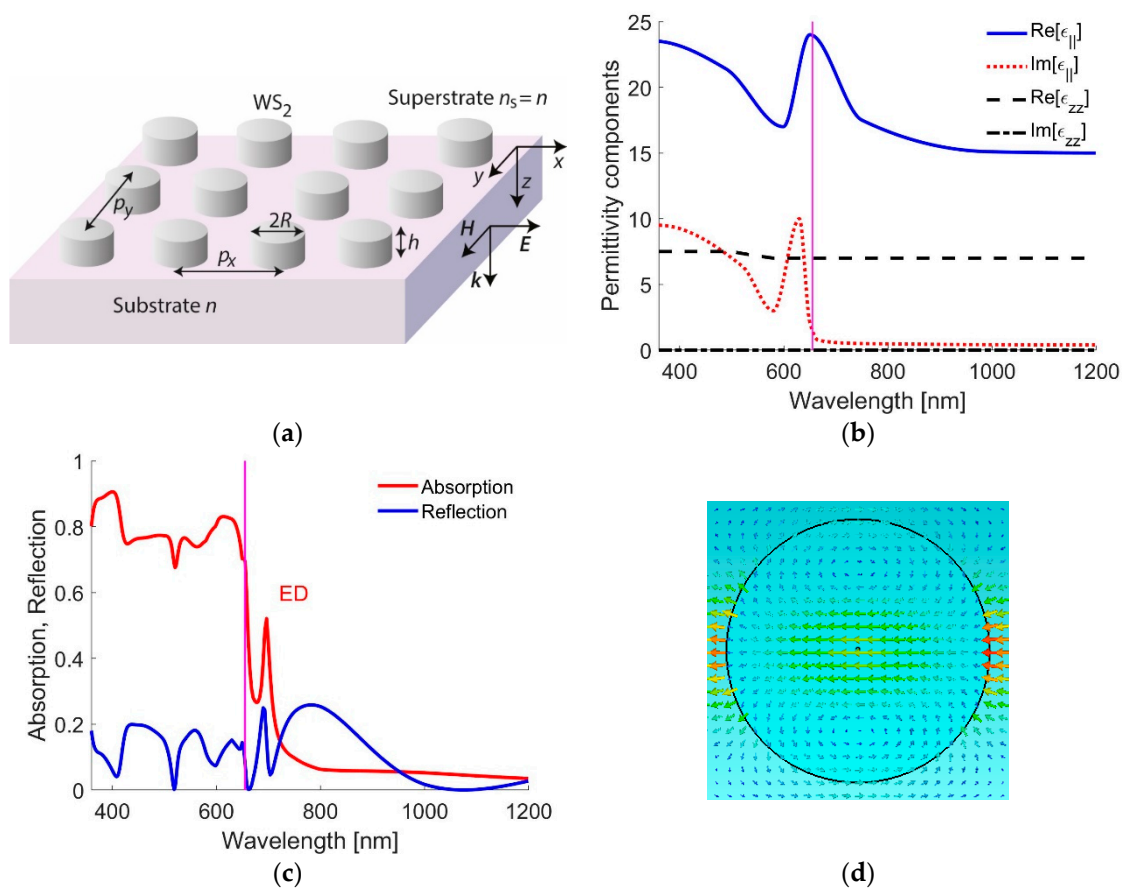


Figure 1. (a) Schematic of the transdimensional lattice under consideration. The parameters are the following: nanodisk radius $R = 100$ nm, height $h = 200$ nm, and refractive index of surrounding $n = n_s = 1.5$. (b) WS₂ permittivity components. (c) Absorption and reflection from the nanoparticle array with periods $p_x = p_y = 240$ nm. Magenta lines on (b) and (c) panels indicate the wavelength λ_c where WS₂ absorption drops significantly, and for $\lambda > \lambda_c$, the nanoparticles support Mie and lattice resonances. (d) E-field distribution at $\lambda = 697$ nm indicating ED contribution of the resonance.

For a spherical particle with isotropic constituent material, each of these periods controls different lattice resonances: under illumination with x -polarized light, p_x controls the magnetic dipole (MD) and electric quadrupole (EQ) resonances, and p_y controls ED and magnetic quadrupole (MQ) [17,24,25]. These considerations are approximately valid for disks even though the description of the particle includes a tensorial polarizability. Calculations in Figure 2 show that under change of p_y , the ED resonance shifts to longer wavelength. In Figure 2, calculation results are terminated at Rayleigh anomaly wavelength $\lambda_{RA} = np_{x,y}$ to account for only sub-diffraction effects. Upon further increase in the period ($p_y > 400$ nm), the ED transforms to ED-lattice-resonance (ED-LR) and follows the Rayleigh anomaly. Even for fairly large periods $p_y > 700$ nm, the resonance is well defined, and one can see peaks in absorption and reflection profiles. Similar to the effect of p_y changes, changes in p_x result in the excitation of lattice resonances in the proximity to the Rayleigh anomaly, but the resonances do not extend to a longer wavelength. This behavior is typical for the nanoparticles with rapidly decreasing polarizability.

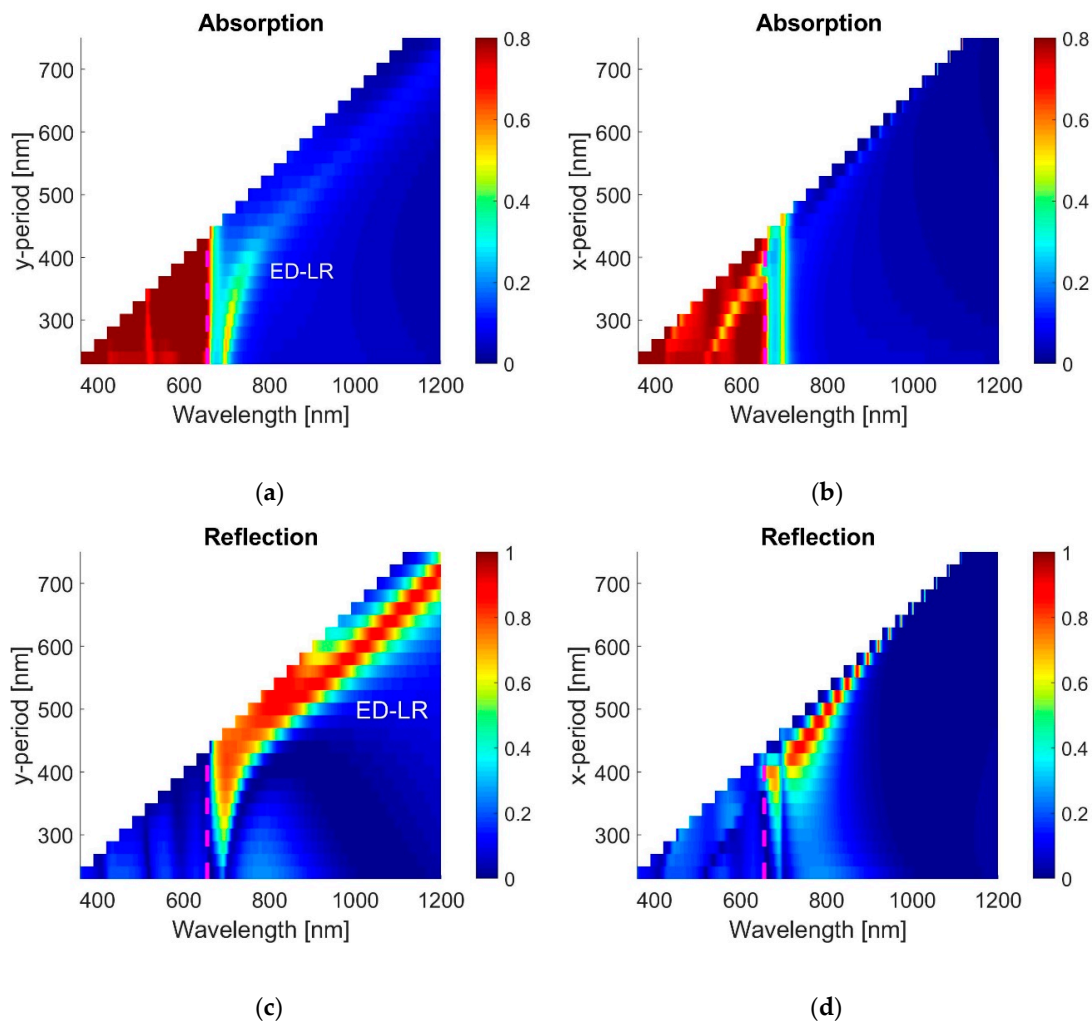


Figure 2. (a,b) Absorption and (c,d) reflection in nanoparticle array for different periods. In (a,c) period p_y changes and $p_x = 240$ nm. In (b,d), period p_x is changes and $p_y = 240$ nm. Magenta dashed lines indicate the same wavelength of absorption drop λ_c as in Figure 1. Electric dipole lattice resonances (ED-LRs) appear for a change of the period p_y , which is in full agreement with the analytical considerations for incident field E along the x -axis. Calculation results are terminated at Rayleigh anomaly wavelength $\lambda_{RA} = np_{x,y}$ to account for only sub-diffraction effects.

3. Conclusions

To sum up, we have studied a transdimensional lattice consisting of a two-dimensional periodic arrangement of WS_2 nanodisks with single-particle Mie resonances defined by disk parameters in all three dimensions. Even though the TMDC family of materials have high permittivity comparable to silicon and III-V materials, the idea of engineering Mie resonances in nanoparticle lattices and designing metasurfaces based on them remain overlooked. In this work, we show that well-defined Mie resonances are not only excited in single or closely packed nanodisks but the resonances can be also shifted by the array periods. Because of the high value of in-plane permittivity component in the visible and near-infrared spectral ranges, the lattice resonances of the electric dipole can be excited even in the elongated lattice and in a broad spectral range.

Author Contributions: Conceptualization, V.E.B. and J.V.M.; Methodology, V.E.B.; Formal Analysis, V.E.B.; Writing-Review and Editing, V.E.B. and J.V.M.; Funding Acquisition, J.V.M.

Acknowledgments: This material is based upon work supported by the Air Force Office of Scientific Research under Grant No. FA9550-19-1-0032.

Conflicts of Interest: The authors declare no conflict of interest. The funders had no role in the design of the study; in the collection, analyses, or interpretation of data; in the writing of the manuscript, and in the decision to publish the results.

References

1. Luk'yanchuk, B.; Zheludev, N.I.; Maier, S.A.; Halas, N.J.; Nordlander, P.; Giessen, H.; Chong, C.T. The Fano Resonance in Plasmonic Nanostructures and Metamaterials. *Nat. Mater.* **2010**, *9*, 707. [[CrossRef](#)] [[PubMed](#)]
2. Babicheva, V. Directional Scattering by the Hyperbolic-Medium Antennas and Silicon Particles. *MRS Adv.* **2018**, *3*, 1913–1917. [[CrossRef](#)]
3. Babicheva, V. Long-Range Propagation of Plasmon and Phonon Polaritons in Hyperbolic-Metamaterial Waveguides. *J. Opt.* **2017**, *19*, 124013. [[CrossRef](#)]
4. Evlyukhin, B.; Novikov, S.M.; Zywiets, U.; Eriksen, R.L.; Reinhardt, C.; Bozhevolnyi, S.I.; Chichkov, B.N. Demonstration of Magnetic Dipole Resonances of Dielectric Nanospheres in the Visible Region. *Nano Lett.* **2012**, *12*, 3749–3755. [[CrossRef](#)] [[PubMed](#)]
5. Person, S.; Jain, M.; Lapin, Z.; Saenz, J.J.; Wicks, G.; Novotny, L. Demonstration of Zero Optical Backscattering from Single Nanoparticles. *Nano Lett.* **2013**, *13*, 1806–1809. [[CrossRef](#)]
6. Fu, Y.H.; Kuznetsov, A.I.; Miroshnichenko, A.E.; Yu, Y.F.; Lukyanchuk, B. Directional Visible Light Scattering by Silicon Nanoparticles. *Nat. Commun.* **2013**, *4*, 1527. [[CrossRef](#)]
7. Babicheva, V.E.; Moloney, J. Lattice Effect Influence on the Electric and Magnetic Dipole Resonance Overlap in a Disk Array. *Nanophotonics* **2018**, *7*, 1663–1668. [[CrossRef](#)]
8. Babicheva, V.E.; Petrov, M.; Baryshnikova, K.; Belov, P. Reflection Compensation Mediated by Electric and Magnetic Resonances of All-Dielectric Metasurfaces [Invited]. *J. Opt. Soc. Am. B* **2017**, *34*, D18–D28. [[CrossRef](#)]
9. Shcherbakov, M.R.; Liu, S.; Zubyuk, V.V.; Vaskin, A.; Vabishchevich, P.P.; Keeler, G.; Pertsch, T.; Dolgova, T.V.; Staude, I.; Brener, I.; et al. Ultrafast All-Optical Tuning of Direct-Gap Semiconductor Metasurfaces. *Nat. Commun.* **2017**, *8*, 17. [[CrossRef](#)]
10. Boltasseva, A.; Shalaev, V.M. Transdimensional Photonics. *ACS Photonics* **2019**, *6*, 1–3. [[CrossRef](#)]
11. Abate, Y.; Gamage, S.; Li, Z.; Babicheva, V.; Javani, M.H.; Wang, H.; Cronin, S.B.; Stockman, M.I. Nanoscopy Reveals Surface-Metallic Black Phosphorus. *Light Sci. Appl.* **2016**, *5*, e16162. [[CrossRef](#)] [[PubMed](#)]
12. Boulesbaa, A.; Babicheva, V.E.; Wang, K.; Kravchenko, I.I.; Lin, M.-W.; Mahjouri-Samani, M.; Jacob, C.; Puretzky, A.A.; Xiao, K.; Ivanov, I.; et al. Ultrafast Dynamics of Metal Plasmons Induced by 2D Semiconductor Excitons in Hybrid Nanostructure Arrays. *ACS Photonics* **2016**, *3*, 2389–2395. [[CrossRef](#)]
13. Babicheva, V.; Gamage, S.; Zhen, L.; Cronin, S.B.; Yakovlev, V.S.; Abate, Y. Near-Field Surface Waves in Few-Layer MoS₂. *ACS Photonics* **2018**, *5*, 2106–2112. [[CrossRef](#)]
14. Babicheva, V.E.; Moloney, J. Lattice Zenneck Modes on Subwavelength Antennas. *Laser Photonics Rev.* **2019**, *13*, 1800267. [[CrossRef](#)]
15. Verre, R.; Baranov, D.G.; Munkhbat, B.; Cuadra, J.; Käll, M.; Shegai, T. Transition Metal Dichalcogenide Nanodisks as High-Index Dielectric Mie Nanoresonators. *Optics* **2018**, *1812*, 04076. [[CrossRef](#)]
16. Dong, R.; Kuljanishvili, I. Review Article: Progress in Fabrication of Transition Metal Dichalcogenides Heterostructure Systems. *J. Vac. Sci. Technol. B Nanotechnol. Microelectron.* **2017**, *35*, 030803. [[CrossRef](#)] [[PubMed](#)]
17. Evlyukhin, A.B.; Reinhardt, C.; Seidel, A.; Luk'yanchuk, B.S.; Chichkov, B.N. Optical Response Features of Si-Nanoparticle Arrays. *Phys. Rev. B* **2010**, *82*, 045404. [[CrossRef](#)]
18. Wang, W.; Ramezani, M.; Vakevainen, A.I.; Torma, P.; Rivas, J.G.; Odom, T.W. The Rich Photonic World of Plasmonic Nanoparticle Arrays. *Mater. Today* **2018**, *21*, 303–314. [[CrossRef](#)]
19. Kravets, V.G.; Kabashin, A.V.; Barnes, W.L.; Grigorenko, A.N. Plasmonic Surface Lattice Resonances: A Review of Properties and Applications. *Chem. Rev.* **2018**, *118*, 5912–5951. [[CrossRef](#)]
20. Zou, S.; Janel, N.; Schatz, G.C. Silver Nanoparticle Array Structures that Produce Remarkably Narrow Plasmon Line Shapes. *J. Chem. Phys.* **2004**, *120*, 10871. [[CrossRef](#)]
21. Markel, V.A. Divergence of Dipole Sums and the Nature of Non-Lorentzian Exponentially Narrow Resonances in One-Dimensional Periodic Arrays of Nanospheres. *J. Phys. B Atom. Mol. Opt. Phys.* **2005**, *38*, L115–L121. [[CrossRef](#)]

22. Zhou, W.; Dridi, M.; Suh, J.Y.; Kim, C.H.; Co, D.T.; Wasielewski, M.R.; Schatz, G.C.; Odom, T.W. Lasing Action in Strongly Coupled Plasmonic Nanocavity Arrays. *Nat. Nanotechnol.* **2013**, *8*, 506–511. [[CrossRef](#)]
23. Zhukovsky, S.V.; Babicheva, V.E.; Uskov, A.V.; Protsenko, I.E.; Lavrinenko, A.V. Electron Photoemission in Plasmonic Nanoparticle Arrays: Analysis of Collective Resonances and Embedding Effects. *Appl. Phys. A* **2014**, *116*, 929–940. [[CrossRef](#)]
24. Evlyukhin, A.B.; Reinhardt, C.; Zywiets, U.; Chichkov, B.N. Collective Resonances in Metal Nanoparticle Arrays with Dipole-Quadrupole Interactions. *Phys. Rev. B* **2012**, *85*, 245411. [[CrossRef](#)]
25. Babicheva, V.E.; Evlyukhin, A.B. Resonant Lattice Kerker Effect in Metasurfaces with Electric and Magnetic Optical Responses. *Laser Photonics Rev.* **2017**, *11*, 1700132. [[CrossRef](#)]
26. Babicheva, V.E. Lattice Effect in Mie-Resonant Dielectric Nanoparticle Array under the Oblique Light Incidence. *MRS Commun.* **2018**, *8*, 1455–1462. [[CrossRef](#)]
27. Babicheva, V.E. Multipole Resonances in Transdimensional Lattices of Plasmonic and Silicon Nanoparticles. *MRS Adv.* **2019**, *4*, 713–722. [[CrossRef](#)]



© 2019 by the authors. Licensee MDPI, Basel, Switzerland. This article is an open access article distributed under the terms and conditions of the Creative Commons Attribution (CC BY) license (<http://creativecommons.org/licenses/by/4.0/>).